Highly selective ultrafast circularly polarized photodiodes based on π-conjugated polymers

Matthew D. Ward[a,b], Jessica Wade[b,c], Xingyuan Shi[b,d], Jenny Nelson[a,b], Alasdair J. Campbell[a,b†], Matthew J. Fuchter[b,d*]

Dedication: *Dedicated to the memory of Professor Alasdair James Campbell*

[a]*Department of Physics, Imperial College London, South Kensington Campus, Prince Consort Road, London SW7 2AZ, UK,* [b]*Centre for Processable Electronics, Imperial College London, South Kensington Campus, London SW7 2AZ, UK,* [c]*Department of Materials, Exhibition Road, Imperial College London, SW7 2AZ,* [d]*Department of Chemistry and Molecular Sciences Research Hub, Imperial College London, White City Campus, 82 Wood Lane, London W12 0BZ, UK*

† Deceased

***e-mail: m.fuchter@imperial.ac.uk**

Keywords

Chiral Materials; Chiroptical Response; Circularly Polarized Light; Organic Photodiodes; Photodetectors

Abstract

Chiral π-conjugated molecular systems that are intrinsically sensitive to the handedness of circularly polarized (CP) light potentially allow for miniaturized, low-cost CP detection devices. Such devices promise to transform several technologies, including biosensing, quantum optics and communication of data encrypted by exploiting the spin angular momentum of light. Here we realize a simple, bilayer organic photodiode (CP OPD) comprising an achiral π-conjugated polymer–chiral additive blend as the electron donor layer and an achiral C_{60} electron acceptor layer. These devices exhibit considerable photocurrent dissymmetry g_{ph}, with absolute values as high as 0.85 and dark currents as low as 10 pA. Impressively, they showcase a linear dynamic range of 80 dB, and rise and fall times of 50 and 270 ns respectively, which significantly outperforms all previously reported CP selective photodetectors. Mechanistically, we show that the g_{ph} is sensitive to the thickness of *both* the chiral donor and achiral

acceptor layers and that a trade-off exists between the external quantum efficiency (EQE) and g_{ph}. The fast-switching speeds of these devices, coupled with their large dynamic range and highly selective response to CP light, opens up the possibility of their direct application in CP sensing and optical communication.

Introduction

Photonic devices that make use of circularly polarized (CP) light will revolutionize the fields of biosensing[1], quantum optics[2,3], polarization-enhanced imaging[4–6], microfluidics[7] and encrypted optical communications [8]. Central to these applications is the ability to discriminate between left- and right-handed CP light (LH CPL and RH CPL hereafter). This is typically achieved by combining an inorganic photodetector and polarizing optical components – a configuration unsuitable for miniaturization or low-cost manufacture. As a result, recent efforts have concentrated on the design of active layers that can intrinsically detect CP light (CPL), eliminating the need for bulky, complex device architectures.

The detection of CPL is primarily achieved in two ways, (1) the manipulation of the local electromagnetic environment with chiral plasmonic nanostructures or (2) the use of chiral molecules in active layers.[9–12] For CP organic photodetectors (OPDs), a common figure of merit used to evaluate the selectivity of their response to the handedness of CPL is the dissymmetry or '*g*-' factor, which is defined as:

$$g = \frac{I_L - I_R}{\frac{1}{2}(I_L + I_R)}$$

Here, subscripts L and R denote LH CPL and RH CPL, respectively, and *I* is either the resultant absorbance or the photocurrent of the device, giving rise to the dissymmetry of absorption, g_{abs}, and dissymmetry of photocurrent, g_{ph}, respectively.[13,14] For OPDs, other important figures of merit include external quantum efficiency (EQE), dark current, rise time (t_{rise}) and fall time (t_{fall}), which are defined in the Supporting Information (SI; Table S1).

The recent research interest in chiral optoelectronic devices has seen the realization of several CP photodetectors based on both organic and organic–inorganic hybrid chiral systems (summarized in Table S1). However, all of these systems have their own shortcomings. While devices that incorporate chiral plasmonic nanostructures can exhibit outstanding CP selectivity ($|g_{ph}| \leq 1.6$), they typically suffer from low EQE (≤ 1%) and cannot operate in the visible spectral region[11,15]. Their widespread

application is further hindered by complex fabrication protocols, which often involve slow instrumentation (e.g. electron-beam lithography) that render the mass production of components a challenge[16]. The device architectures that demonstrate the greatest CP selectivity (i.e., approaching $|g_{ph}| \sim 2$, perfect CP selectivity) are based on the field-effect transistor (FET) structure, but these devices suffer from low EQE ($\sim 10^{-2}$ %) and cannot be scaled up.[10,17,18] Chiral hybrid organic-inorganic perovskite (HOIP) photodetectors have achieved impressive EQEs (~57%), but unfortunately, the majority of published devices demonstrate poor CP selectivity ($|g_{ph}| \sim 0.1$).[19–21] More recently, a low-dimensional chiral HOIP has been reported that allows for high CP selectivity in the UV ($|g_{ph}| = 1.9$).[22] Such perovskite devices face challenges relative to competitive technologies however, such as toxicity and instability. While a handful of chiral OPDs have been reported, they demonstrate modest values of $|g_{ph}|$ (≤ 0.1), and other crucial figures of merit (e.g. EQE, linear dynamic range and response times) are rarely disclosed.[9,12,14]

Chiral π-conjugated organic systems can demonstrate large g_{abs}, as well as offering tunable optoelectronic properties and compatibility with flexible substrates. In such systems, the dissymmetric photocurrent originates from the dissymmetric absorption of the materials, which can be quantified by their circular dichroism (CD). Photoactive achiral polymer–chiral additive blends constitute a particularly attractive and versatile class, demonstrating large g_{abs} and enabling polymers that have been optimized for photodetection to be re-purposed for CP discrimination without the need for novel synthesis efforts. Recently, Kim *et al.* combined the achiral polymer poly[3-(6-carboxyhexyl)thiophene-2,5-diyl] (P3CT) with the chiral additive 1,1′-binaphthyl to realize a CP photodiode ($|g_{ph}| = 0.1$, EQE = 18%). Unfortunately, the very slow fall times of these devices (>250 s) makes them practically unsuitable in any frequency-domain applications.[12] Our group and others have demonstrated high-efficiency, high-dissymmetry ($|g_{EL}| \approx 1.1$) CP organic light-emitting diodes (OLEDs) based on achiral polyfluorene-based (co)-polymers blended with a chiral small-molecule (1-aza[6]helicene, hereafter aza[6]H) additive.[23–25] We have since postulated that the origins of these chiroptical phenomena lie in the formation of a weakly ordered double-twist cylinder blue phase, where

the aza[6]H serves to template the polymers into twisted fibrils with strong magneto-electric coupling.[26]

Here we report the realization of highly selective CP OPDs based on a simple, planar heterojunction architecture comprising a poly(9,9-dioctylfluorene-*alt*-bithiophene) (F8T2):aza[6]H blend electron donor layer and a C_{60} electron acceptor layer. To the best of our knowledge, these devices represent the highest photocurrent dissymmetry ever reported for a CP OPD ($|g_{ph}|$= 0.72 at zero bias), along with ultrafast response times ($t_{rise} \approx 50$ ns; $t_{fall} \approx 270$ ns) that are four orders of magnitude faster than those reported for all other CP photodetecting devices. Such fast responses open up the possibility of using these devices for short range visible light communication.[27] These devices represent the first CP OPDs with device performance compatible with the demands of real-world technologies and, through mechanistic device analysis, emphasize the importance of both π-conjugated polymer structure and device architecture in the ability to differentiate LH and RH CP light.

Results

The use of thermal annealing to induce a giant chiroptical response in F8T2:aza[6]H blends has already been evaluated by our group, and, unless stated otherwise, we followed the optimized protocol (140 °C for 10 minutes in a N_2 filled glovebox) for all experiments.[26] The naming convention for LH−CPL and RH−CPL is illustrated in the SI (Figure S1). To ensure that the chiral phase is not impacted by the subsequent deposition of the C_{60} layer, we compared the CD spectra of donor-only thin films (F8T2:aza[6]H) to those obtained for the donor-acceptor (D–A) bilayer heterojunction (F8T2:aza[6]H–C_{60}), and find no evidence of the thermally evaporated C_{60} layer disrupting the formation of the chiral phase (Figure S2).

We first fabricated a series of CP OPDs (of device structure ITO/PEDOT:PSS/F8T2:aza[6]H/C_{60}/Al; Figure 1) with variable F8T2:aza[6]H thickness (t_D of 77–140 nm) and a fixed C_{60} layer thickness (t_A = 30 nm). Details of experimental setups for device measurements are provided in the SI (Figure S3). We previously showed that when considering thick films (t_D >150 nm) the true g_{abs} of our annealed blend materials does not vary with thickness.[26] The

same does not hold true for the thin films (t_D <150 nm) evaluated here, which we attribute to the strong optical interference of forward and backward traversing waves caused by multiple reflections at the substrate–film and other neighboring layers' interfaces, typical of optically thin films.[28] The CD (Figure 1b), as well as the apparent $|g_{abs}|$ (Figure S4), increases with increasing t_D and are equal-and-opposite for [*M*]- and [*P*]-aza[6]H blends.[26] Irrespective of the polarization of the excitation, the EQE decreases as t_D increases (Figure 1c). As can be expected from the increasing g_{abs}, $|g_{ph}|$ values corresponding to the spectral region of first CD Cotton band (~480 nm) increase with increasing t_D, from ~0.15 at t_D = 81 nm to ~0.41 for t_D = 110 nm (shown in Figure 1d case of an [*M*]-aza[6]H-doped CP OPD). We note that g_{ph} is of opposite handedness relative to the corresponding g_{abs}; that is, donor layers that preferentially absorb RH CPL result in a higher EQE under LH CPL near the D–A interface, and *vice versa*. Under reverse bias (Figures 1e and 1f) the CP OPDs demonstrate an enhanced g_{ph}; for example, when t_D = 140 nm, $|g_{ph}|$ increases from 0.3 (unbiased) to 0.85 (−3 V).

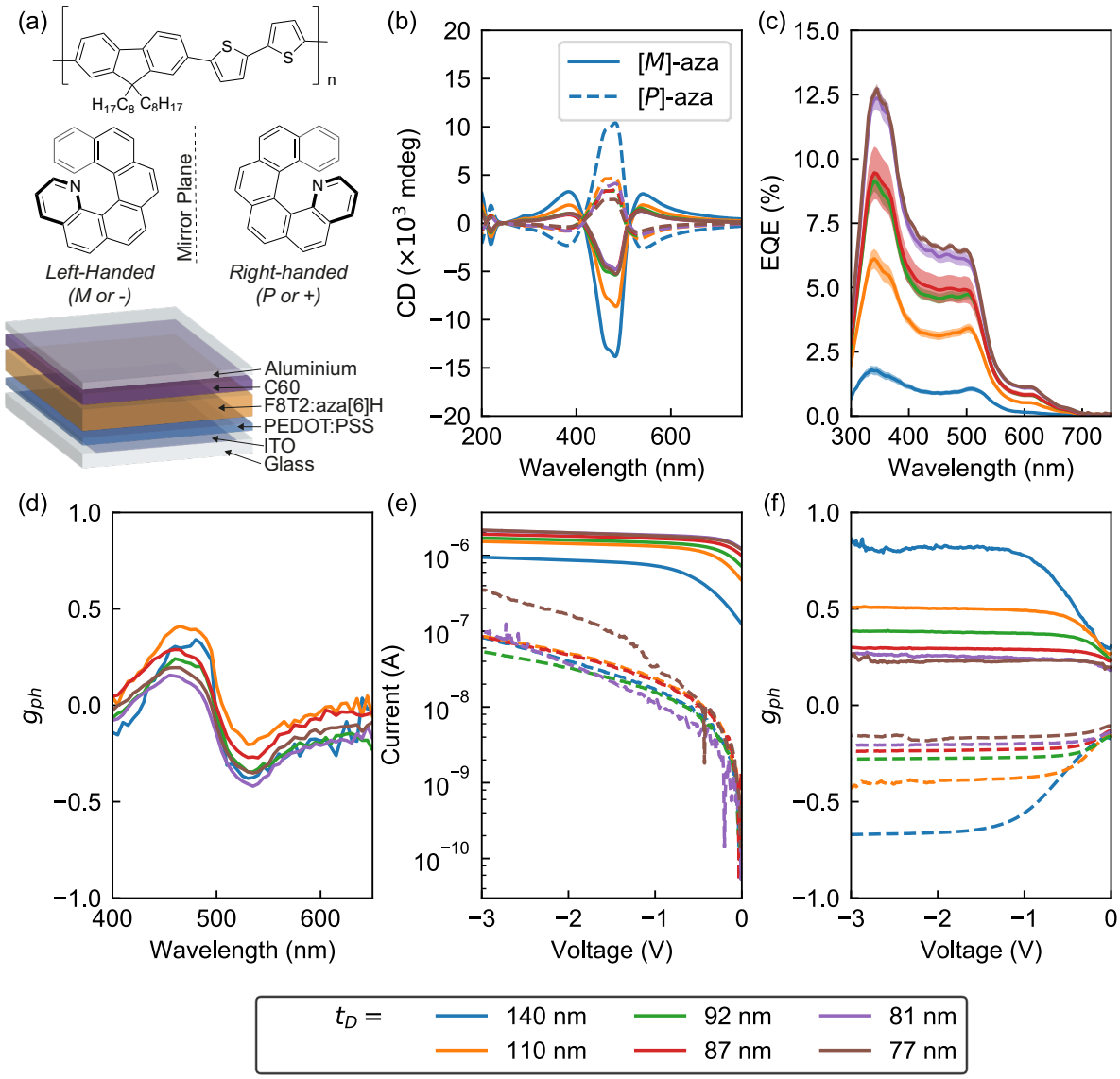

Figure 1. Influence of the blend donor layer thickness, t_D, on CP OPD performance while keeping the acceptor layer thickness at 30 nm. (**a**) Molecular structures of F8T2 (top), [*M*]-aza[6]H and [*P*]-aza[6]H (middle), and the OPD architecture (bottom). (**b**) CD of F8T2:[*M*]- (solid) and [*P*]-aza[6]H (dashed) blend layers. (**c**) Unpolarized EQE and (**d**) g_{ph} for F8T2:[*M*]-aza[6]H OPDs at 0 V bias; varying weights of curves in (c) represents instrumentational error margins in EQE data. (**e**) Current–voltage curves of F8T2:[*M*]-aza[6]H based OPDs under dark conditions (dashed) and unpolarized light (solid; with incident radiation 0.55 mW cm^{-2}, λ_{ex} = 473 nm). (**f**) g_{ph} of F8T2:[*M*]-aza[6]H (solid) and F8T2:[*P*]-aza[6]H (dashed) OPDs under reverse bias (0.21 mW cm^{-2}, λ_{ex} = 473 nm).

Next, we evaluated the impact of the C_{60} layer (t_A = 0–50 nm) on the device performance, using a fixed t_D (77 nm). At all excitation wavelengths probed, EQE initially increases with increasing t_A (Figure 2a), until $t_A \geq 40$ nm, when the EQE falls sharply (from ~8% to ~3% for λ >400 nm). Unexpectedly, short circuit $|g_{ph}|$ for the longer-wavelength peak (corresponding to the CD peak at around 540 nm) increases as t_A decreases (Figure 2b), reaching $|g_{ph}| \approx 0.72$ when t_A = 10 nm. This increase is coupled with a blue shift of the wavelength (λ_{ph}) at which the maximum $|g_{ph}|$ occurs (λ_{ph} ~540 nm at t_A of 50 nm, λ_{ph} ~510 nm at t_A of 10 nm). The relationship between g_{ph} and t_A is particularly surprising given that the presence of the achiral acceptor layer does not significantly impact the CD response (Figure S2). We note that there is no significant enhancement of photocurrent or g_{ph} under increasing reverse bias (Figures 2c and d).

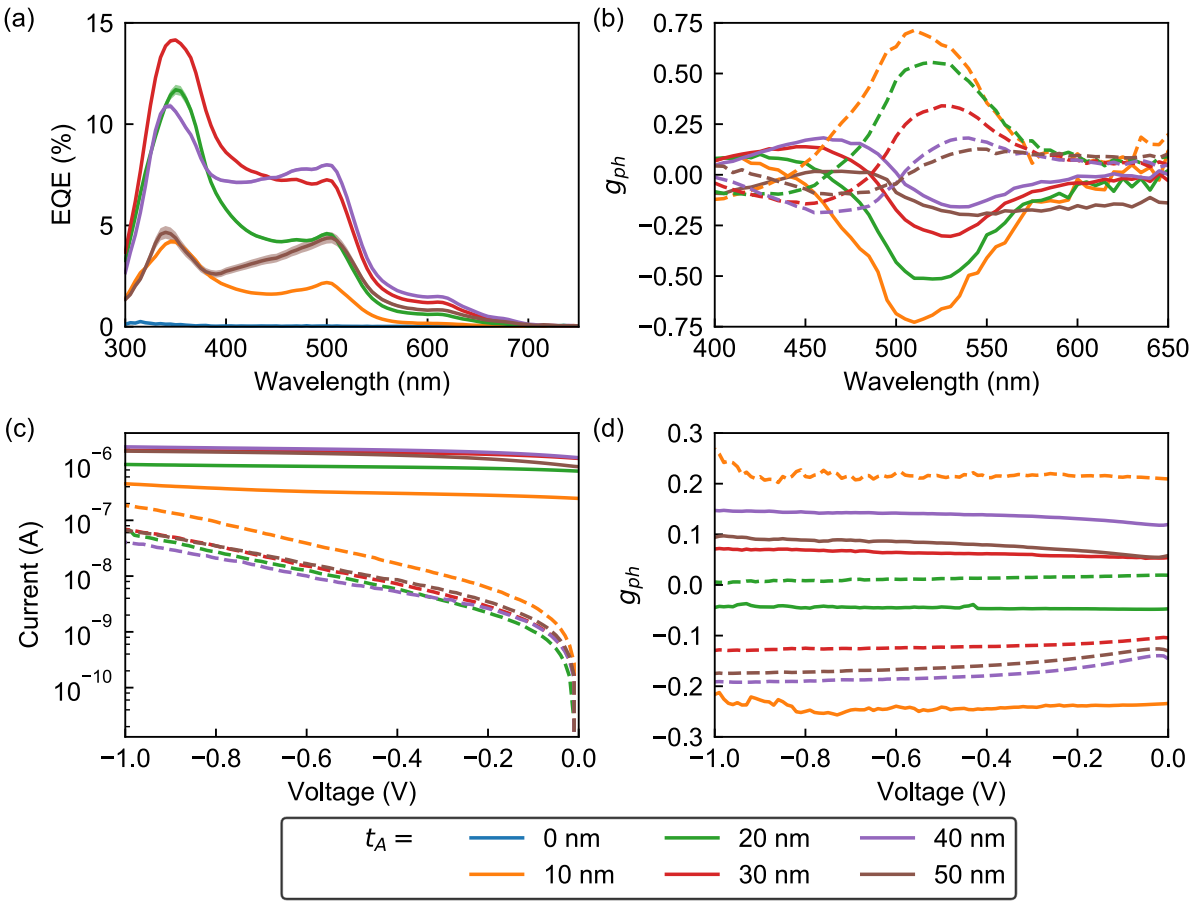

Figure 2. Influence of C_{60} acceptor layer thickness, t_A, on CP OPD performance with a fixed donor layer thickness of 77 nm. (**a**) Unpolarized EQE and (**b**) g_{ph} for F8T2:[*M*]- (solid) and [*P*]-aza[6]H (dashed) OPDs at zero bias. (**c**) Current–voltage curves of F8T2:[*M*]-aza[6]H devices under dark

conditions (dashed) and unpolarized light (solid; with incident radiation 0.57 mW cm^{-2}, λ_{ex} = 473 nm). (**d**) g_{ph} of F8T2:[*M*]-aza[6]H (solid) and F8T2:[*P*]-aza[6]H (dashed) OPDs under reverse bias (0.22 mW cm^{-2}, λ_{ex} = 473 nm).

Given the trends we observed as a function of t_D and t_A, we selected two device architectures for further study: one targeting the most intense, first Cotton CD band ('**1**', λ = 480 nm; with t_D = 87 nm and t_A = 30 nm) and the other targeting the longer-wavelength CD band ('**2**', λ = 540 nm; t_D = 77 nm and t_A = 20 nm). These architectures maximize the difference in EQE under LH CPL and RH CPL at their target wavelengths in order to optimize both EQE and g_{ph}. In both cases, the EQE (Figure 3a) and g_{ph} (Figure 3b) are enhanced under reverse bias, reaching $|g_{ph}|$ >0.4 at an EQE of 8.4% for band **1** and $|g_{ph}|$ >0.1 at an EQE of 5.2% for band **2**. Both devices exhibit a linear response to increasing light intensity (λ_{ex} = 473 nm) of over four orders of magnitude (Figures 3c and d), yielding linear dynamic range (LDR) values of ~80 dB, and similar ultrafast response times under pulsed operation (t_{rise} ~50 ns and t_{fall} ~270 ns).

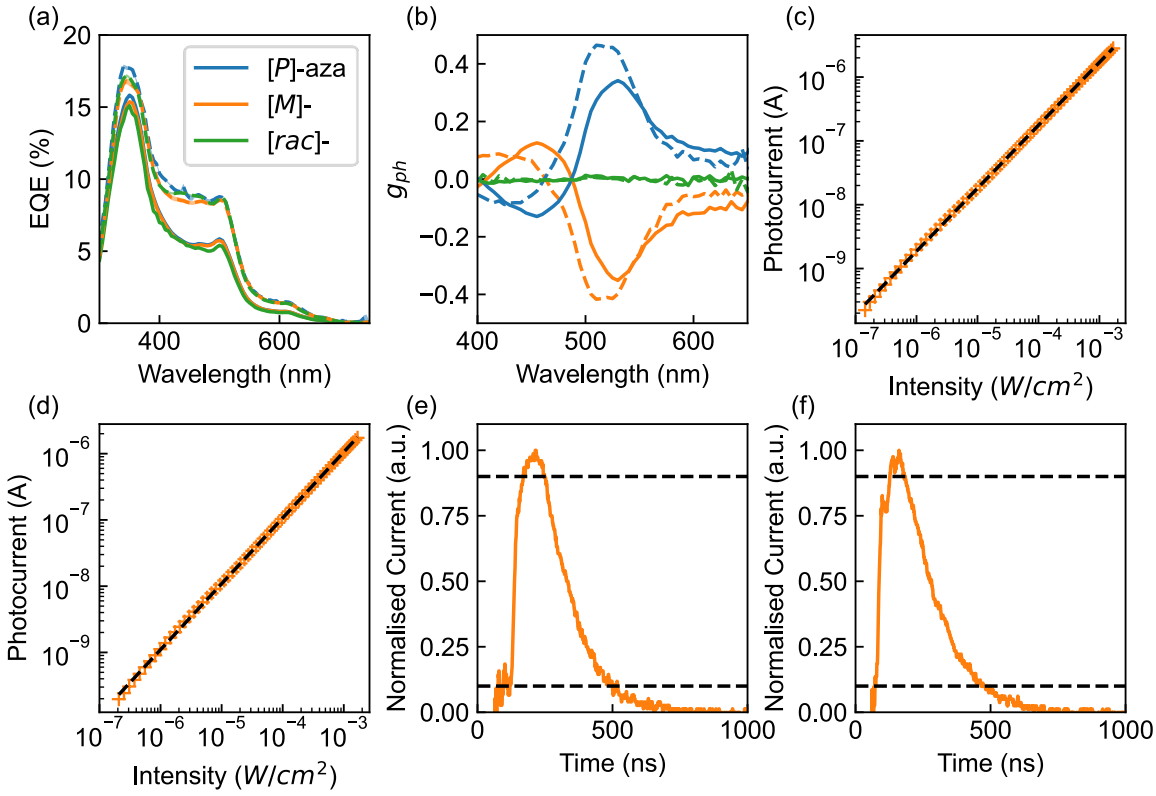

Figure 3. Device characteristics of optimized OPDs incorporating [*M*]-, [*P*]- or [*rac*]-aza[6]H chiral dopants. (**a**) Unpolarized EQE and (**b**) g_{ph} for OPDs fine-tuned for operation in CD band **1** (solid, −1 V) or CD band **2** (dashed, −0.5 V). Unpolarized LDR of (**c**) band **1**-oriented OPDs and (**d**) band **2**-oriented OPDs, where dashed lines indicate the line of best fit. Non-CP switching response of (**e**) band **1** and (**f**) band **2** OPDs, where dashed lines indicate 10% and 90% of the maximum current. Incident radiation λ_{ex} = 473 nm for obtaining (c) and (d); and λ_{ex} = 532 nm used for (e) and (f).

These results not only showcase the first example of the versatile achiral polymer–chiral small-molecule additive blend systems in CP OPDs but also provide a simple platform to understand the fundamental mechanisms that underpin their device performance. The decrease in EQE with increasing t_D (Figure 1b) can be understood by considering the photogeneration and subsequent dissociation of excitons. As t_D is considerably greater than the exciton diffusion length of F8T2 (~8 nm), one can assume to a first approximation that statistically, most excitons generated in the donor layer more than ~8 nm from the D–A interface would not dissociate before annihilation, and therefore do not contribute to the measured photocurrent.[29] As t_D increases, the proportion of incident photons that are absorbed before they reach the D–A interface increases, and the resulting reduced light intensity at the D–A interface diminishes the EQE. On the other hand, g_{ph} increases with increasing t_D, and is always opposite in sign to g_{abs} (Figures 1b, d and f). This behavior has previously been observed using a planar heterojunction architecture by Meskers and co-workers, and can be explained by considering the mechanism illustrated in Figure 4a.[9] For F8T2:[*M*]-aza[6]H devices, RH CPL is more strongly absorbed than LH CPL in the donor layer. As a result, the intensity of light that reaches the D–A interface is greater for LH CPL than it is for RH CPL, which leads to an inversion of g_{ph} relative to g_{abs}. As t_D is increased, this 'filter' effect is further enhanced, which serves to increase $|g_{ph}|$. The enhancement of $|g_{ph}|$ under reverse bias, which is particularly apparent when t_D is high (Figure 1f), suggests that the efficiency of either exciton generation, exciton dissociation or charge extraction does not increase equally with reverse bias under LH and RH CPL. Further studies are required to elucidate the precise origins of this interesting phenomenon.

While increasing t_D has a detrimental impact on device performance, the same is not true for the achiral acceptor layer (t_A) (Figures 2a and c). Consistent with an exciton diffusion length of ~40 nm for C_{60}, EQE and photocurrent increase until t_A = 40 nm, i.e., a length until which most excitons can diffuse to the D–A interface thus contribute to the photocurrent.[29] When the C_{60} acceptor layer thickness exceeds the exciton diffusion length (t_A >40 nm), EQE and photocurrent decrease sharply. We attribute this to the absorption of light in the excessively thick C_{60} layer, which non-selectively reduces the light intensity that is reflected to and beyond the D–A interface from the aluminum electrode. At the same time, when the CP OPDs are excited in the low-energy CD band (~540 nm), $|g_{ph}|$ is dramatically enhanced by decreasing t_A (Figures 2b and d). We suggest that this behavior is the result of two cooperative mechanisms (Figure 4b). As described above, for F8T2:[*M*]-aza[6]H devices, circular selective absorption of RH CPL results in a greater $|g_{ph}|$ under LH CPL. The LH CPL transmitted through the achiral C_{60} layer is reflected off the back aluminum electrode, after which the handedness inverts (LH becomes RH, and *vice versa*). Following reflection, the CPL is the appropriate handedness to be preferentially absorbed by the chiral donor layer near the heterojunction interface. As t_A decreases, the amount of light transmitted through the acceptor layer increases, which ultimately increases g_{ph}. We attribute the lack of significant enhancement of $|g_{ph}|$ in the high-energy CD band (**1**) to the stronger absorbance of C_{60} at this wavelength (Figure S5). The effect of internal reflection of CPL from the back metallic electrode has also been noted in some CP OLED device works.[30] There is an important difference between the two scenarios however: in CP OLEDs, reflection from the back electrode decreases the dissymmetry factor of CP emission, whereas in CP OPDs it increases the dissymmetry factor of CP detection.

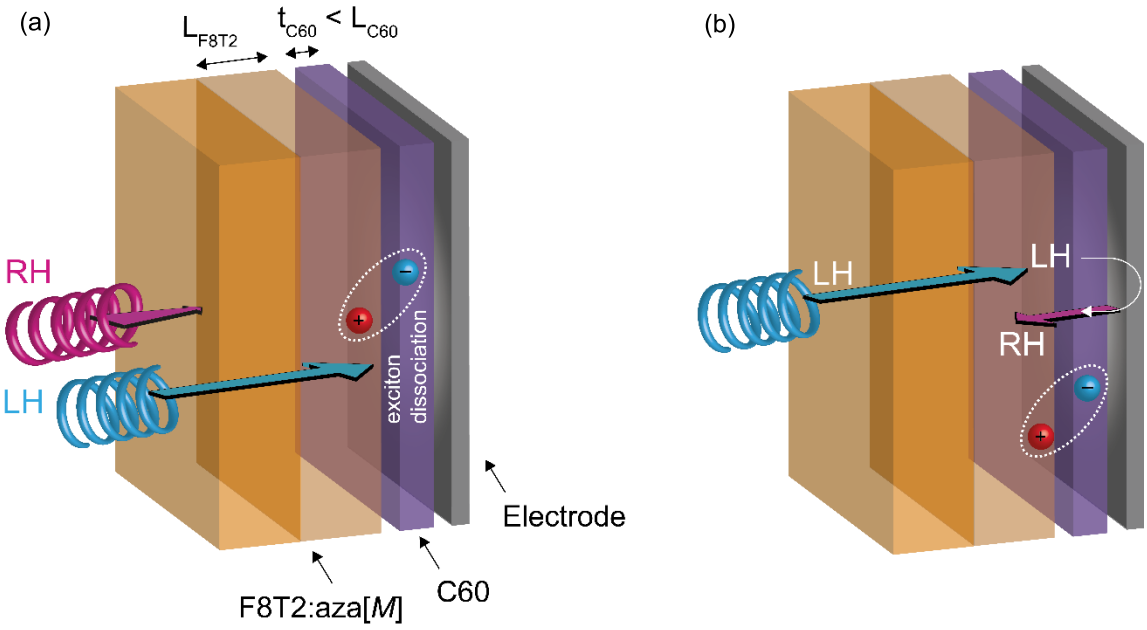

Figure 4. Proposed mechanism for the influence of (**a**) t_D and (**b**) t_A on CP OPD performance. For F8T2:[*M*]-aza[6]H devices, RH CPL is more strongly absorbed than LH CPL in the donor layer, therefore, the intensity of light that reaches the D–A interface is greater under LH CPL than RH CPL, which leads to an inversion of g_{ph} relative to g_{abs}. For thin t_A layers, the LH CPL transmitted through the achiral C_{60} layer is reflected off the back aluminum electrode, after which the handedness inverts (LH becomes RH, and *vice versa*). Following reflection, the CPL is of the appropriate handedness to be more preferentially absorbed by the chiral donor layer near the interface.

The optimized devices represent an ideal balance between device performance and CP selectivity (Figure 3; Table S1). To the best of our knowledge, these devices exhibit the highest LDRs (~80 dB) and fastest switching times (t_{rise} ~50 ns; t_{fall} ~270 ns) of any CP OPDs ever reported. In particular, our switching times are over four orders of magnitude faster (by fall time)[20] than those reported in literature (Table S1). We note that the response times of our CP OPDs correspond to a bandwidth of ~7 MHz. Therefore, these CP OPDs could be used in principle in conjunction with short fluorescence lifetime emitters for high speed wireless visible light communications; with two 7 MHz CPL transmission channels (LH and RH) offering a total transmission bandwidth of up to 14 MHz.[31] Alongside increasing the speed of data transmission, the use of CPL adds an additional degree of

freedom for information encryption, as any eavesdroppers using unpolarized photodetectors will only detect a meaningless superposition of LH CPL and RH CPL signals.

Conclusion

We present highly selective circularly polarized organic photodiodes with state-of-the-art device performance based on a chiral π-conjugated polymer donor and an achiral C_{60} acceptor in a bi-layered planar heterojunction. The simplicity of this architecture allows us to investigate several interesting photophysical and chiroptical phenomena, the findings of which can inform the design of future CP-relevant materials and devices. For example, CP absorption in the donor phase and subsequent inversion upon reflection at the metallic counter electrode results in oppositely handed g_{ph} and g_{abs}. Meanwhile, g_{ph} is largest for the thinnest acceptor layers (g_{ph} = 0.72 when t_A= 10 nm), which we attribute to the beneficial impact of CPL inversion on the photocurrent that is greatest for the thinnest acceptor layers.

This study emphasizes that in the pursuit of high-performance, high-selectivity planar heterojunction CP OPDs, a compromise must be reached between intense g_{ph} and strong EQE. Despite this, our optimized devices demonstrate impressive figures of merit, with EQE of 5–10%, rise and fall times of ~50 ns and ~270 ns, dark currents down to 10 pA, and state-of-the-art linear dynamic ranges of ~80 dB. The strong CP selectivity, coupled with very fast response times has the potential to transform many real-world applications, including CP-light encrypted, ultrafast next-generation data transmission technologies such as visible light communications.

Supporting Information

Supporting Information is available from the Wiley Online Library or from the author.

Acknowledgements

The authors thank the Engineering and Physical Science Research Council for funding through grants EP/L016702/1, EP/R00188X/1 and EP/S515085/1. We would also like to thank the Worshipful Company of Scientific Instrument Makers for additional funding through the WCSIM Postgraduate Scholarship. Prof. Jenny Nelson acknowledges support from the European Research Council (ERC)

under the European Union's Horizon 2020 research and innovation program (grant 742708, CAPaCITy). The authors would also like to acknowledge the contributions of Dr. Jochen Brandt in the purification of F8T2 for the preliminary studies of this device architecture.

Conflict of Interest

The authors declare the following competing financial interest(s): A. Campbell and M. Fuchter are inventors on a patent concerning chiral blend materials (WO2014016611).

References

[1] V. V. Dremin, D. Anin, O. Sieryi, M. A. Borovkova, J. Näpänkangas, I. V. Meglinski, A. V. Bykov, in *Tissue Opt. Photonics* (Eds.: Z. Zalevsky, V. V. Tuchin, W.C. Blondel), **2020**, p. 3.

[2] C. Wagenknecht, C.-M. Li, A. Reingruber, X.-H. Bao, A. Goebel, Y.-A. Chen, Q. Zhang, K. Chen, J.-W. Pan, *Nat. Photonics* **2010**, *4*, 549.

[3] J. F. Sherson, H. Krauter, R. K. Olsson, B. Julsgaard, K. Hammerer, I. Cirac, E. S. Polzik, *Nature* **2006**, *443*, 557.

[4] S. S. Lin, K. M. Yemelyanov, E. N. Pugh, N. Engheta, in *Conf. Proceeding - IEEE Int. Conf. Networking, Sens. Control*, **2004**, pp. 216–221.

[5] S. Peña-Gutiérrez, M. Ballesta, S. Royo, SPIE-Intl Soc Optical Eng, **2019**, p. 38.

[6] J. S. Tyo, M. P. Rowe, E. N. Pugh, N. Engheta, *Appl. Opt.* **1996**, *35*, 1855.

[7] J. Leach, H. Mushfique, R. Di Leonardo, M. Padgett, J. Cooper, *Lab Chip* **2006**, *6*, 735.

[8] P. R. Sura, M. Sekhar, *IETE J. Res.* **2021**, DOI 10.1080/03772063.2020.1871423.

[9] J. Gilot, R. Abbel, C. Lakhwani, E. W. Meijer, A. P. H. J. Schenning, S. C. J. Meskers, *Adv. Mater.* **2010**, *22*, E131.

[10] Y. Yang, R. C. Da Costa, M. J. Fuchter, A. J. Campbell, *Nat. Photonics* **2013**, *7*, 634.

[11] W. Li, Z. J. Coppens, L. V. Besteiro, W. Wang, A. O. Govorov, J. Valentine, *Nat. Commun.*

2015, *6*, 1.

[12] N. Y. Kim, J. Kyhm, H. Han, S. J. Kim, J. Ahn, D. K. Hwang, H. W. Jang, B. K. Ju, J. A. Lim, *Adv. Funct. Mater.* **2019**, *29*, 1808668.

[13] N. Berova, L. Di Bari, G. Pescitelli, *Chem. Soc. Rev.* **2007**, *36*, 914.

[14] M. Schulz, F. Balzer, D. Scheunemann, O. Arteaga, A. Lützen, S. C. J. J. Meskers, M. Schiek, *Adv. Funct. Mater.* **2019**, *29*, 1900684.

[15] J. Peng, B. P. Cumming, M. Gu, *Opt. Lett.* **2019**, *44*, 2998.

[16] T. R. Groves, in *Nanolithography Art Fabr. Nanoelectron. Nanophotonic Devices Syst.*, Elsevier Ltd, **2013**, pp. 80–115.

[17] J. Cheng, F. Ge, C. Zhang, Y. Kuai, P. Hou, Y. Xiang, D. Zhang, L. Qiu, Q. Zhang, G. Zou, *J. Mater. Chem. C* **2020**, *8*, 9271.

[18] W. Shi, F. Salerno, M. D. Ward, A. Santana-Bonilla, J. Wade, X. Hou, T. Liu, T. J. S. Dennis, A. J. Campbell, K. E. Jelfs, M. J. Fuchter, *Adv. Mater.* **2021**, *33*, 2004115.

[19] C. Chen, L. Gao, W. Gao, C. Ge, X. Du, Z. Li, Y. Yang, G. Niu, J. Tang, *Nat. Commun.* **2019**, *10*, 1927.

[20] L. Wang, Y. Xue, M. Cui, Y. Huang, H. Xu, C. Qin, J. Yang, H. Dai, M. Yuan, *Angew. Chemie Int. Ed.* **2020**, *59*, 6442.

[21] D. Li, X. Liu, W. Wu, Y. Peng, S. Zhao, L. Li, M. Hong, J. Luo, *Angew. Chemie - Int. Ed.* **2021**, *60*, 8415.

[22] A. Ishii, T. Miyasaka, *Sci. Adv.* **2020**, *6*, 3274.

[23] D.-M. Lee, J.-W. Song, Y.-J. Lee, C.-J. Yu, J.-H. Kim, *Adv. Mater.* **2017**, *29*, 1700907.

[24] Y. Yang, R. C. da Costa, D.-M. Smilgies, A. J. Campbell, M. J. Fuchter, *Adv. Mater.* **2013**, *25*, 2624.

[25] L. Wan, J. Wade, F. Salerno, O. Arteaga, B. Laidlaw, X. Wang, T. Penfold, M. J. Fuchter, A. J. Campbell, *ACS Nano* **2019**, *13*, 8099.

[26] J. Wade, J. N. Hilfiker, J. R. Brandt, L. Liirò-Peluso, L. Wan, X. Shi, F. Salerno, S. T. J. Ryan, S. Schöche, O. Arteaga, T. Jávorfi, G. Siligardi, C. Wang, D. B. Amabilino, P. H. Beton, A. J. Campbell, M. J. Fuchter, *Nat. Commun.* **2020**, *11*, 1.

[27] H. Haas, L. Yin, Y. Wang, C. Chen, *J. Light. Technol.* **2016**, *34*, 1533.

[28] A. Armin, M. Hambsch, I. K. Kim, P. L. Burn, P. Meredith, E. B. Namdas, *Laser Photon. Rev.* **2014**, *8*, 924.

[29] O. V. Mikhnenko, P. W. M. Blom, T. Q. Nguyen, *Energy Environ. Sci.* **2015**, *8*, 1867.

[30] F. Zinna, U. Giovanella, L. Di Bari, *Adv. Mater.* **2015**, *27*, 1791.

[31] A. L. Kanibolotsky, N. Laurand, M. D. Dawson, G. A. Turnbull, I. D. W. Samuel, P. J. Skabara, *Acc. Chem. Res.* **2019**, *52*, 1665.

TOC entry

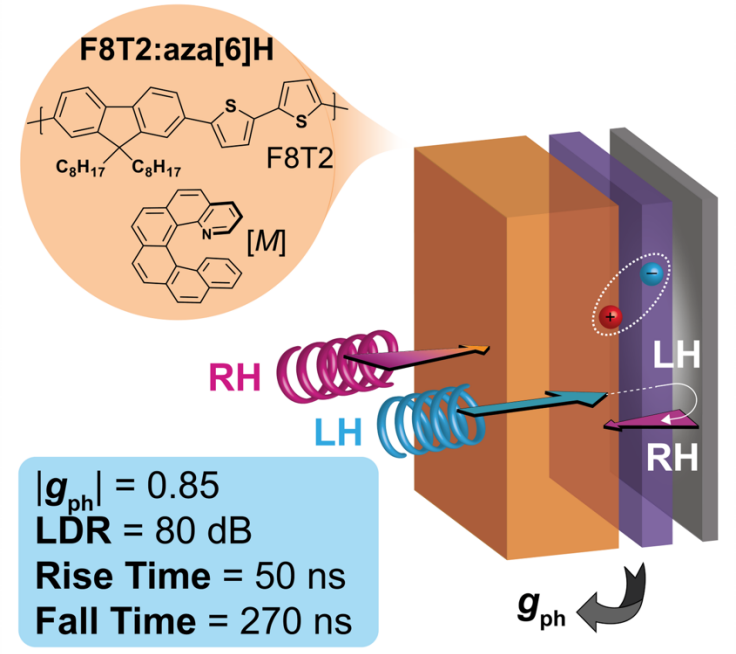

Bilayer organic photodiodes sensitive to the handedness of circularly polarized light (CPL) have been developed using a π-conjugated polymer–chiral additive blend donor layer. The influence of device architecture on the selectivity of response to CPL is leveraged to produce optimized devices with considerable photocurrent dissymmetry (up to 0.85), state-of-the-art linear dynamic range (80 dB), and nanosecond response times.